Islamic University Journal of Applied Sciences (IUJAS)
https://journals.iu.edu.sa/jesc

Volume VIII, Issue I, July 2026, Pages 62-77

Hydrodynamic Behavior of Offset Jets Under Various Situations

Mohammed Awdah B Alshehre[1], Amani Amamou[2, 3], Ali Assoudi[2], H. I. Elsaeedy[1] and Nejla Mahjoub Said[1, *]

[1]Department of Physics, College of Science, King Khalid University, Abha, 61413, Saudi Arabia
445818821@kku.edu.sa, halsayede@kku.edu.sa, nalmahjoub@kku.edu.sa

[2]LGM, National Engineering School of Monastir, University of Monastir, 5000 Monastir, Tunisia

[3]National Engineering School of Gasfa, University of Gafsa, 2112 Gafsa, Tunisia
amani.amamou@yahoo.fr

*Corresponding author: (Nejla Mahjoub Said), *Email Address*: nalmahjoub@kku.edu.sa

Abstract

In this paper, experimental and numerical results of three-dimensional turbulent offset jet flows are investigated through different situations. Velocity measurements are carried out using Laser Doppler Velocimetry (LDV) technique. Numerical simulations are performed by solving the Navier-Stokes equations with the finite volume method using the Reynolds Stress Model (RSM). The different situations of the offset jet are examined; the single offset jet (SOJ), the offset in coflow stream and the dual jet (DJ), for an offset ratio OR = 4 for the SOJ and OR = 0.5 for the DJ configuration. Flow field evolution and hydrodynamic features are presented. It is found that the behavior of the offset jet varies from one situation to another, leading to that the interaction between the offset jet and its surroundings influences the mean velocity decay and the dispersion of the jet flow.

Keywords: Offset jet; Dual jet; Turbulence; Numerical simulation.

https://doi.org/10.63070/jesc.2026.017
Received 18 November 2025; Revised 24 December 2025; Accepted 10 February 2026.
Available online 04 March 2026.
Published by Islamic University of Madinah on behalf of *Islamic University Journal of Applied Sciences*.
This is an open access article published under the Creative Commons Attribution 4.0 International license (CC BY 4.0):https://creativecommons.org/licenses/by/4.0/

1. Introduction

A jet is generated when a fluid is discharged into an ambient medium through a nozzle or orifice with an ejection velocity U_j. The majority of the flows found in nature and engineering applications are turbulent jets. Therefore, considerable researches on jet flows has been conducted in the last few decades to better understand their turbulent behavior and its impact on heat and mass transfer. An offset jet flow is formed by the ejection of a fluid from a nozzle exit into an ambient medium at a certain distance from the boundary surface. The proximity of the jet to the surface influences the dynamic behavior of the flow [1]. The structure of the offset jet flow is described by three different regions. In the first region, the entrainment of the ambient fluid creates a low-pressure zone under the jet due to the presence of the wall. This causes the jet to deviate towards the wall surface and possibly attach to it to form a recirculation zone upstream of the impingement point. The velocity of the jet decreases as it approaches the impingement surface, which allows the pressure inside the jet to increase until it reaches its maximum value at the attachment point. Beyond this point, the pressure gradually decreases along the wall, and the jet continues to develop to form a wall jet.

Many parameters may influence the behavior of an offset jet flow. In early studies [2-5], the reattachment length has usually been the primary parameter of interest to study the characteristics of an offset jet flow. Experimental measurements were made with different techniques such as hotwires, Pitot tubes, Laser Doppler Anemometry (LDA) and Particle Image Velocimetry (PIV). Agelin-chaabet al. [6] examined the effects of the offset ratio (OR) that designed the ratio between the offset height and the nozzle width (h/w), and the Reynolds number on the structure of the turbulent round offset jet using the Particle Image Velocimetry (PIV) at three different Reynolds numbers of 5000, 10000 and 20000. They found that the decay and spread rates are nearly independent of the Reynolds number and the offset height.

Recent numerical investigations [7-9] explored heat transfer enhancement in offset jet configurations using different control strategies. Ajmi et al. [7-8] and Rathore and Verma [9] conducted numerical investigations of turbulent offset jet flows to assess how the jet inclination angle, Reynolds number, and offset ratio influence fluid dynamics and heat transfer. Simulations were performed using CFD with the SST k–ω turbulence model. Results show that increasing the jet obliquity and Reynolds number enhances both local and average Nusselt numbers, while a lower offset ratio improves thermal performance, providing insights for optimizing heating and cooling jet designs. They indicated that offset jet heat transfer can be improved through either jet orientation control or surface geometry modification. Behera and Rathore [10] used CFD with a low-Reynolds-number turbulence model to examine conjugate heat transfer of a turbulent offset jet impinging on a moving flat plate, accounting

for both fluid convection and solid conduction. Results show that smaller offset ratios and higher plate-to-jet velocity ratios enhance the Nusselt number, highlighting the influence of plate motion and geometry on convective cooling performance. Mele et al. [11] analyzed flow and heat transfer in a plate with embedded discrete heaters cooled by a turbulent offset jet through steady-state convection–conduction simulations. The study highlights that material properties and heater configurations strongly influence conjugate heat transfer in plates cooled by turbulent offset jets. They observed that polymer plates experience higher heat transfer but greater thermal gradients, while ceramic plates exhibit lower and more uniform heating. In addition to RANS-based studies, more recent LES simulations of a planar offset wall-jet [12, 13] (Choudhury A. R., Anupindi; Hossen et al.) were conducted. Choudhury and Anupindi [12] provided higher-fidelity insight into turbulence dynamics, showing three peaks in the streamwise Nusselt number and highlighting enhanced heat transfer in the recirculation region, for Re = 7500 and an offset ratio OR = 5. In the case of sinusoidal pulsating offset jet, Aghaei et al. [14] numerically investigated turbulent sinusoidally pulsating offset jets, showing that low-frequency, small-amplitude oscillations enhance heat transfer and significantly influence thermal performance.

A recent experimental study by Nyantekyi-Kwakye [15] examined the flow development and turbulence characteristics of turbulent offset jets issuing from sharp-edged rectangular nozzles. Velocity and turbulence statistics were obtained using Acoustic Doppler Velocimetry (ADV), revealing the role of nozzle geometry and expansion conditions on jet decay, recirculation, large-scale vortex structures, and mixing behavior. Complementing these findings, Hakimi and Khorsandi [16] investigated turbulent round offset jets in quiescent and coflowing environments, showing that coflow modifies jet spreading, decay rates, and turbulence intensity, providing further insights into how external conditions influence offset jet flow development and entrainment. The Coandă effect is investigated in shallow-water free surface offset jets by Sollevanti et al. [17], extending classic air-jet studies to hydraulically relevant conditions. The paper experimentally shows that free-surface dynamics enhance jet attachment, yielding shorter reattachment lengths, and proposes simple scaling laws that unify jet behavior across flow regimes.

The combination between an offset jet and a wall jet is refers to as dual jet (DJ). Murphy et al. [18-20] conducted experimental studies of wall-bounded dual jets. First, they investigated [8] the effects of velocity ratio ($R = U_j/U_\infty = 0.5–2$), Reynolds number (Re = 5500–12,000) and offset ratio using infrared thermography and Particle Image Velocimetry (PIV). They found that for $R < 1$, the offset jet dominated while for $R > 1$, the wall jet constrained the offset jet and stabilized the flow. Likewise, the heat transfer is shown to be strongly influenced by R. Then, Murphy et al. [20] validated their

experimental setup by comparing a single wall jet and a single offset jet results with results from literature. By using PIV measurements, a dual jet flow field is investigated for Reynolds numbers ranging from 5500 to 12000, with an offset ratio and a velocity ratio equal to the unity. They concluded that the rising of Re leads to a slight reduction in the size of the recirculation region together with the increase of the defection of both jets. The study of Altaharwah and Hsu [21] investigated dual parallel plane jets with a fixed offset ratio. They used smoke visualization and hot-wire measurements to examine how Reynolds number ratios between the two jets and pulsation control flow interaction and mixing influence the dynamics of dual plane jets. Results show that varying the Reynolds ratio changes the dominant jet, significantly affecting lateral spreading, turbulence, and overall mixing efficiency. Kumar and Murugan [22] extended previous analyses by using PIV to capture the full velocity field and coherent flow structures of the interacting jets. Mondal et al. [23] investigated the behavior of a dual jet with and without a parallel co-flow stream, using the standard k–ω turbulence model. They focused on how the co-flow velocity (CFV) affects heat transfer when the bottom wall is kept at a constant temperature. The authors found that increasing the co-flow velocity weakens the heat transfer in dual jet systems, mainly by lowering the Nusselt number in the merging region. However, Xu et al. [24] used realizable k–ε model and transient PISO solver to investigate the energy separation phenomenon in the shear layer of two parallel free air jets under a range of Reynolds numbers. Results show that increasing Reynolds number intensifies thermal separation, while jet interaction geometry partially suppresses the effect.

Based on the over-mentioned rsearches, single offset and dual jet configurations have been extensively studied, whether experimentally or numerically. However, this paper aims to proof the use of a single offset jet with a jet density $\rho_j = 1.3$ and an offset ratio $OR = h/d_h = 4$ by ARECO group (ARECO®: Air Refreshing Control) as a specific application for nebulisation to preserve freshness and nutritional qualities of vegetables. In fact, d_h is hydraulic diameter and h is the jet offset height for SOJ and refers to the separation distance between the two parallel jet for the dual jet arrangement. The present paper investigates the behavior of a three-dimensional turbulent plane offset jet injected under different situations and combines experimental measurements and numerical simulations. Experiments are conducted using a Laser Doppler Velocimetry (LDV) technique for the SOJ case. Computations are performed with the Ansys-Fluent software using the RSM model and applied on a non-uniform grid mesh selected after a carful mesh sensibility test for both SOJ and DJ cases. The maximum mean velocity decay along the axial direction and the vertical distributions of the axial mean velocity in the plane of symmetry ($z = 0$) for different streamwise locations and for different velocity ratios are investigated.

2. Experimental and numerical set-up

2.1 Experimental set-up

Experimental measurements are conducted in a test section of 1500mm × 400mm × 400mm in the longitudinal, vertical and lateral directions, respectively (Figure 1).

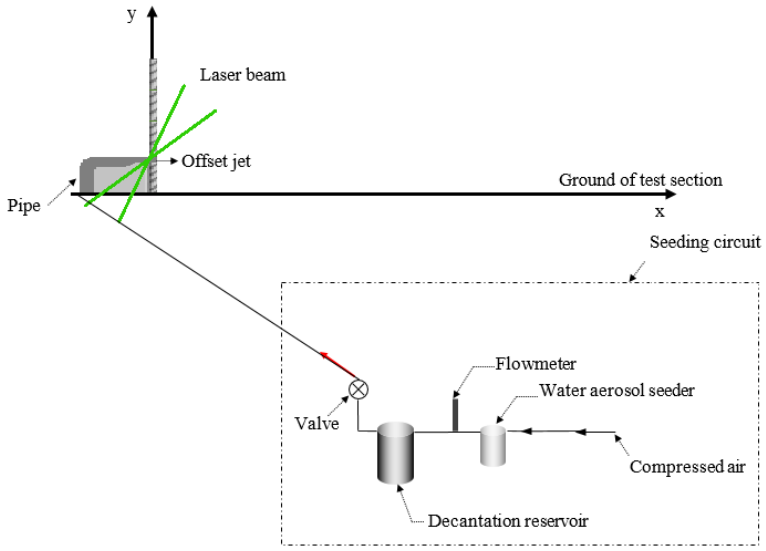


Figure 1. Skeleton view of the experimental setup

The jet flow is discharged from a rectangular nozzle (L×w) with an offset height h above the horizontal wall. Test section specifications are recapitulated in Table 1.

Table 1. Test section specifications

Parameter	Value
Nozzle dimension (mm²)	L×w = 30×6
Offset height (mm)	h = 40
Jet hydraulic diameter (mm)	d_h = 10

The Laser Tomography System (LTS), for the flow visualization, and the Laser Doppler Velocimetry (LDV) technique, for the velocity measurements, are used to investigate the flow structure. The jet is formed by an airflow seeded with small particles of water cloud of approximately 3µm diameter

(Nebulization, ARECO®: Air Refreshing Control). LDV system specifications are resumed in Table 2.

Table 2. LDV system specifications

Parameter	**Specification**
LDV type	Three-component LDV
Laser operation mode	Monochromatic laser
Scattering configuration	Optical probe volume at beam intersection
Seeding method	Nebulization
Seeding material	Water droplets (aerosol)
Seeding particle diameter	3 µm
Data processing software	FLOWSIZER

2.2 Numerical set-up

The flow is assumed steady, incompressible, turbulent and three-dimensional. The averaged equations describing the behavior of the offset jet flow is written as:

$$\frac{\partial U_i}{\partial x_i} = 0 \tag{1}$$

$$\frac{\partial}{\partial x_k}(U_k U_i) = -\frac{1}{\rho}\frac{\partial P}{\partial x_i} + \frac{\partial}{\partial x_k}\left[\nu\left(\frac{\partial U_i}{\partial x_k} + \frac{\partial U_k}{\partial x_i}\right) - \overline{u_i' u_k'}\right] \tag{2}$$

Where $i, k = 1, 2, 3$ referring to x, y and z respectively. $\overline{u_i' u_k'}$ are the Reynolds stresses terms. The closure turbulence model RSM (Reynolds Stress model) is used to solve this system of equations.

$$\underbrace{\frac{\partial}{\partial x_k}(U_k \overline{U_i' U_j'})}_{C_{ij}} = \underbrace{\frac{\partial}{\partial x_k}\nu\frac{\partial}{\partial x_k}(\overline{U_i' U_j'})}_{D_{ij}^L} - \underbrace{\left[\overline{U_i' U_k'}\frac{\partial U_j}{\partial x_k} + \overline{U_j' U_k'}\frac{\partial U_i}{\partial x_k}\right]}_{P_{ij}} + D_{ij}^T + G_{ij} + \phi_{ij} + \varepsilon_{ij} \tag{3}$$

C_{ij} denotes the convective term and D_{ij}^L, P_{ij}, D_{ij}^T, G_{ij}, φ_{ij}, ε_{ij}, represent respectively, the molecular diffusion, the stress production, the turbulent diffusion, the buoyancy production, the pressure strain and the dissipation rate [10]. The equation of the turbulent kinetic energy (k) and that of the dissipation rate of the kinetic energy (ε) which are relative to the second-order model are defined as follows [25]:

$$U_i \frac{\partial K}{\partial x_i} = \frac{\partial}{\partial x_k}\left[\left(\nu + \frac{\nu_t}{\sigma_k}\right)\frac{\partial k}{\partial x_k}\right] + \frac{1}{2}P_{ii} - \varepsilon \tag{4}$$

$$U_i \frac{\partial \varepsilon}{\partial x_i} = \frac{\partial}{\partial x_k}\left[\left(\nu + \frac{\nu_t}{\sigma_\varepsilon}\right)\frac{\partial \varepsilon}{\partial x_k}\right] + C_{\varepsilon 1}\frac{1}{2}P_{ii}\frac{\varepsilon}{k} - C_{\varepsilon 2}\frac{\varepsilon^2}{k} \quad (5)$$

where $C_{\varepsilon 1} = 1.44, C_{\varepsilon 2} = 1.92$ and $\sigma_\varepsilon = 1$.

The governing equations, along with the corresponding boundary conditions (Table 3) and imposed experimental values (Table 4), are solved using the CFD software Ansys Fluent [26] based on the Finite Volume Method (FVM). The discretization of the equations is carried out using a first-order upwind scheme. The SIMPLE algorithm is employed to ensure proper coupling between pressure and velocity fields. The resulting algebraic equations are solved iteratively through the Tri-Diagonal Matrix Algorithm (TDMA). The absolute convergence criterion was established by requiring the residuals of the continuity and momentum equations to fall below. After satisfying this requirement, the same threshold was subsequently applied to the energy equation, ensuring complete convergence of the coupled flow and thermal fields.

Table 3. Boundary conditions details

Boundaries	**Velocity**
Offset jet inlet	$u = U_j, v = 0, w = 0$
External flow	$u = U_\infty, v = 0, w = 0$
Vertical wall	$u = 0, v = 0, w = 0$
Horizontal wall	$u = 0, v = 0, w = 0$
Rest of the domain	$\frac{\partial u}{\partial n} = 0, \frac{\partial v}{\partial n} = 0, \frac{\partial w}{\partial n} = 0$

Table 4. Experimental conditions details

Parameter	**Value**
Jet exit velocity (m s^{-1})	Uj = 3.4
Jet density (kg/m^3)	ρ_j = 1.3
Reynolds number (-)	Re_j = 2455

The experimental set-up, described above, is reproduced fairly using the CFD procedure. Figure 2 illustrates a mesh sensitivity study based on the maximum velocity decay (U_m/U_j) for a SOJ. Several computational grids are evaluated to examine the influence of mesh resolution on the numerical results confronted to present experimental data for OR = 4. Four representative grids are reported in this study

varying from coarse to very fine meshes. As shown in Figure 2, the normalized maximum velocity decay obtained with Mesh 3 and Mesh 4 closely matches the experimental data. Therefore, Mesh 3 is considered sufficiently refined to yield grid-independent predicted results. After this careful grid independence investigation, the picked out grid is 1.3×10^6 cells with details reported in Table 5.

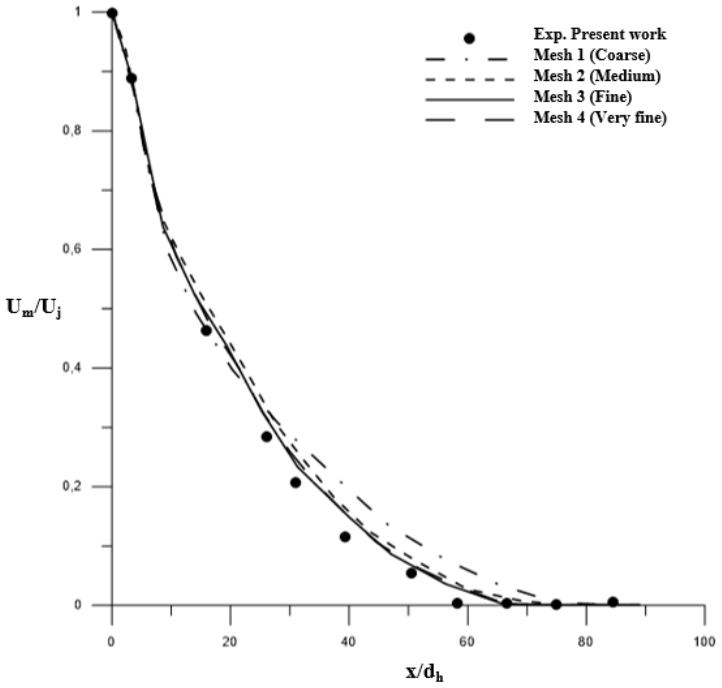


Figure 2. Grid independence test

Table 5. Grid details

n_x	n_y	n_z	y^+	Total cells
180	90	80	$30 < y^+ < 100$	$1.3\ 10^{-6}$

3. Results and discussion

3.1 Single offset jet

The evolution of a single offset jet (SOJ) with a density of $\rho_j = 1.3$ is presented in Figure 3 for OR = 4. In the symmetry plane (z = 0), the jet emerges and diffuses through the ambient surrounding immediately downstream of the nozzle exit. The jet is deflected and rolled up, causing the formation of shear layer vortices (SLV). In the near field, the offset height seems to influence the development

of the jet indicated by the breakdown of the flow after a short axial distance downstream of the nozzle exit. This breakdown leads to the attachment of the jet to the bottom wall, located in the impingement point.

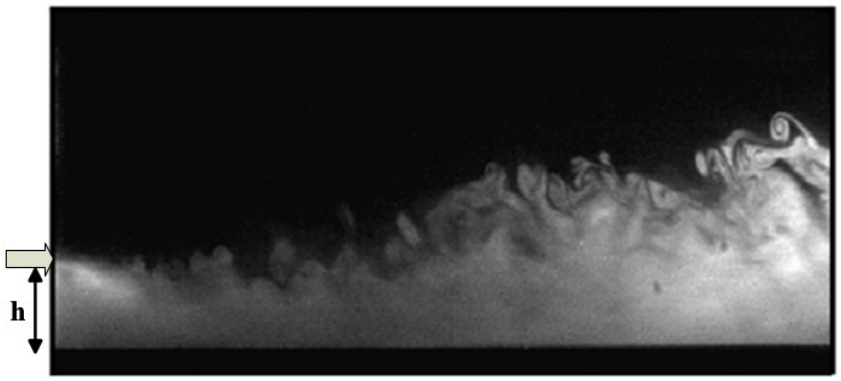


Figure 3. Flow visualization in the symmetry plane for OR = 4

The variation of the maximum velocity normalized by the jet velocity (U_m/U_j) is plotted along the normalized axial direction (x/d_h) in Figure 4. Experimental data from Agelin-Chaab and Tachie [6] are considered for comparison together with present LDV experimental measurements. It is obvious that the two curves follows the same decay beginning with a higher initial decrease in the near jet exit region. A small discrepancy is observed between the present experimental measurements and those reported by Agelin-Chaab and Tachie [6]. This difference may be attributed to the use of different jet fluids: a water jet in [6] and an air jet in the present experiments. Predicted results fairly follow both experimental data. Further downstream, the effect of the offset height is notable, when the offset height is smaller, the maximum velocity decays rapidly.

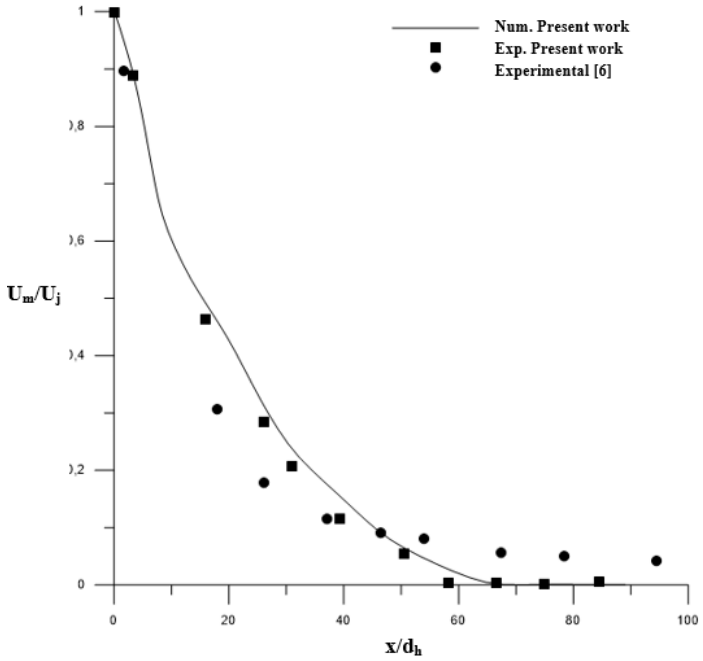


Figure 4. Maximum mean velocity decay

3.2 Offset jet into coflow stream

The air jet flow is discharged from a vertical wall offset by a height h above the horizontal wall with an ejection velocity U_j into an external flow, in coflow direction, stagnant or with a uniform velocity U_∞. The vertical distributions of the axial mean velocity component in the plane of symmetry (z = 0) for different streamwise locations ($x/d_h = 4$, $x/d_h = 7$ and $x/d_h = 10$) and for different velocity ratios (R = 1, R< 1, R > 1) are shown in Figure 5.

It is clear that, downstream of the jet nozzle exit, the profiles of the normalized axial velocity (U/U_m) exhibit negative values near the horizontal wall for the three velocity ratios pointing out the presence of a recirculation zone. This considered region is marked by the presence of vortices in contrast with the case where the offset jet is emerged in quiescent ambient; $R = \infty$ [27]. Moving vertically away from the nozzle exit, the mean axial velocity increases with the normalized vertical coordinate (y/d_h) to reach the uniform velocity of the external fluid leading to the maximum value $U/U_m = 1$, far from the interaction zone. Besides the presence of an external flow stream in coflow direction influences the parameters of the offset jet (the reattachment length and the attachment point), it is found that increasing the coflow velocity (i.e. the velocity ratio decreases) leads to the decrease of the mean axial velocity.

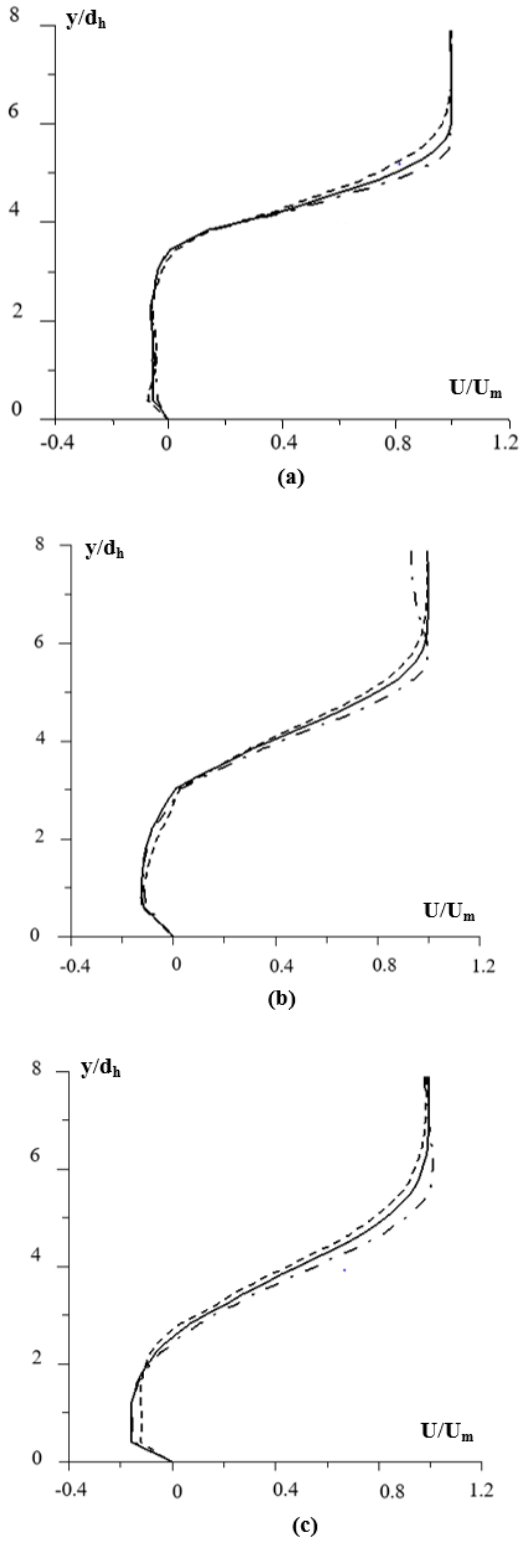


Figure 5. Axial mean velocity profiles for different velocity ratios at various streamwise positions (a) $x/d_h = 4$, (b) $x/d_h = 7$, (c) $x/d_h = 10$

3.3 Dual jet

The evolution of a single offset jet (SOJ) and a dual jet (DJ) at an OR = 0.5 is illustrated through the streamlines of axial velocity in the Figure 6 (a) and Figure 6 (b), respectively. The most remarkable observation is the pronounced recirculation region below the jet in the case of a single offset jet and between the two nozzles of two parallel plane jets. This leads to determine the reattachment point (rp) for a SOJ, defined as the first point on the impingement wall where the fluid attaches, and the merging point (mp) for a DJ at which the two jets deflect to each other and merge together. There two characteristic points are presented in Figure 6 (a) and Figure 6 (b), respectively. It is found that the merging point is located at $x_{mp}/d_h = 9.3$ and the reattachment point is situated at $x_{rp}/d_h = 11.5$.

The DJ flow is characterized by two vortices rotating in opposite directions inside the recirculation zone, opposite the SOJ flow, where only one vortex is formed in the recirculation zone between the nozzle and the impingement surface. Furthermore, it is observed that the SOJ's recirculation region is larger than that of DJ, resulting that the locus of the reattachment point is far from the merging point.

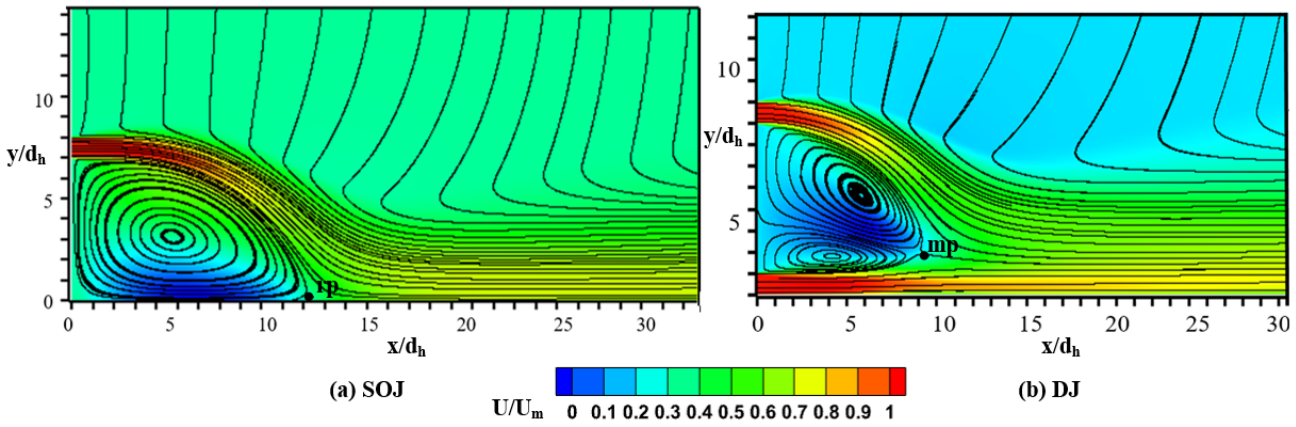


Figure 6. Streamlines of axial velocity of (a) a single offset jet and (b) a dual jet

Figure 7 exhibits the predicted maximum velocity decays of both single offset jet (SOJ) and dual jet (DJ) confronted to experimental data of Wang and Tan [28]. The normalized maximum velocity remains constant for few hydraulic diameters downstream of the nozzle exit and then decreases gradually whilst moving away from the initial jet region. It is worth noting that the maximum velocity in the case of DJ decays more rapid than that of SOJ in the converging zone (the near flow field) due to the strong interaction between the two parallel jets. These indicates that the SOJ potential core is larger than that of DJ. Downstream the initial region, the both jet configurations show similar decay rate except that the maximum velocity in the case of SOJ decreases faster than that in the case of DJ.

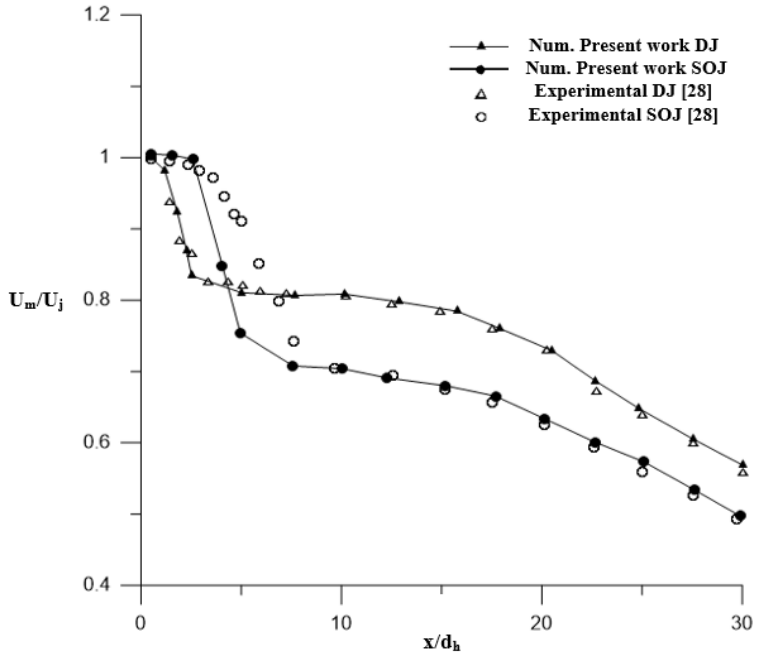


Figure 7. Normalized velocity decay of a dual jet compared to that of a single offset jet for OR = 0.5

4. Conclusion

An experimental and computational study has been carried out to investigate the hydrodynamic behavior of the offset jet configuration under various situations; a single offset jet, an offset jet into coflow stream and a dual jet. Experimental data are measured with Laser Doppler Velocimetry (LDV) technique for the single offset jet and numerical results are predicted using the CFD software Ansys-Fluent for both single offset jet and dual jet configurations. The study addresses an industrially relevant topic by investigating the application of an offset jet within the ARECO nebulization system as a strategy to reduce food waste.

The comparison between experimental and predicted results as well as data from literature exhibits good agreement. It is clear that the offset height has a notable influence on the maximum velocity decay showing that smaller offset height leads to rapid maximum velocity decay. In the presence of a coflow stream, increasing the coflow velocity (i.e., decreasing the velocity ratio) leads to a reduction in the mean axial velocity. Numerical results illustrate the formation of a recirculation zone beneath the jet for the single offset jet and between the two nozzles for the dual parallel plane jets, with the recirculation region being larger in the single offset jet configuration. Furthermore, the potential core of the single offset jet is longer than that of the dual jet, resulting in a more rapid decay of the maximum velocity for the dual jet in the near-field region.

Funding

The authors declare that this research received no external funding.

Data Availability Statement

Not applicable.

Conflicts of Interest

There is no conflict of interest, the writers assert.

References

[1] A. Assoudi, A. Amamou, N.M. Said, H. Bournot, Characteristics and analysis of a turbulent offset jet including the effect of density and offset height, Int. J. Mech. Sci. 174 (2020) 105477.

[2] D.I. McRee, H.L. Moses, The effect of aspect ratio and offset ratio on nozzle flow and jet reattachment, in: Advances in fluids, F.T. Brown (Eds.), ASME Press, New York, 1967, pp. 142-161.

[3] N. Rajaratnam, K. Subramanya, Plane turbulent reattached wall jets, J. Hydraul. Div. 94 (1968) 95-112.

[4] J. Hoch, L.M. Jiji, Theoretical and experimental temperature distribution in two-dimensional turbulent jet boundary interaction, J. Heat Transf. 103 (1981) 331-335.

[5] A. Nasr, J. Lai, A turbulent plane offset jet with small offset ratio. Exp. Fluid. 24 (1998) 47–57.

[6] M. Agelin-Chaab, M.F. Tachie Characteristics and structure of turbulent 3D offset jets, Int. J. Heat Fluid Flow. 32:3https://www.sciencedirect.com/journal/international-journal-of-heat-and-fluid-flow/vol/32/issue/3 (2011) 608-620.

[7] M. Ajmi, N. Hnaien, S. Marzouk, L. Kolsi, K. Ghachem, H. Ben Aissia, M.A. Almeshaal, Numerical investigation of heat transfer enhancement of an inclined heated offset jet. Int. Commun. Heat Mass Transf. 116 (2020) 104682.

[8] M. Ajmi, N. Hnaien, S. Marzouk, L. Kolsi, K. Ghachem, H. Ben Aissia, Numerical investigation and triple-parameters correlations development on the dynamic characteristics of a turbulent offset jet, J. Turbul. 22:6 (2021) 325-352.

[9] S.S. Rathore, S.K. Verma, Numerical investigation on the efficacy of jet obliquity for fluid flow and thermal characteristics of turbulent offset jet, Heat Mass Transf. 58 (2022) 1223–1246.

[10] V.M. Behera, S.K. Rathore, The effect of plate motion on heat transfer enhancement using turbulent offset jet flow: A conjugate approach, Int. Commun. Heat Mass Transf. 136 (2022) 106173.

[11] B. Mele, G. Ruocco, Conjugate heat transfer from a discrete-source heated plate by offset jet impingement, Int. J. Heat Mass Transf. 217 (2023) 124651.

[12] A.R. Choudhury, K. Anupindi, LES of a planar offset wall jet with heat transfer-characterization, turbulent kinetic energy and Reynolds shear stress budgets, Int. J. Heat Mass Transf. 191 (2022) 122847.

[13] M.K. Hossen, E. Asgari, M. Saeedi, B. Nyantekyi-Kwakye, Large-eddy simulation of an offset jet flow over surface-mounted ribs. Proc. CSME Congress, Canada, 2025.

[14] A. Aghaei, S. Jahangiri, A.I. Khdair, R.S. Faisal, M. Afrand, Investigation of turbulent heat transfer in sinusoidal pulsating offset jets: a numerical study, Int. J. Therm. Sci. 220 (2026) 110427.

[15] B. Nyantekyi-Kwakye, Large-scale motion of submerged offset jets issuing from sharp-edged rectangular nozzles, Proc. Inst. Mech. Eng. Part C J. Mech. Eng. Sci. 235:1 (2020) 78-93.

[16] F. Hakimi, B. Khorsandi, Dynamics of round turbulent offset jets in quiescent and coflowing environments, Phys. Fluid. 36 (2024) 105156.

[17] M. Sollevanti, M. Miozzi, G.P. Romano, Coandă effect in free-surface shallow-water offset jets. Exp. Fluids. 66 (2025) 57.

[18] P.J. Murphy, S. Alimohammadi, S.M. O'Shaughnessy An experimental investigation of the effect of the velocity ratio on the flow and wall heat transfer characteristics of a wall-bounded dual jet. Therm. Sci. Eng. Progress. 66 (2025) 104007.

[19] P.J. Murphy, S. Alimohammadi, S.M. O'Shaughnessy, Experimental investigation of the effect of the offset ratio on the flow characteristics and heat transfer behaviour of a wall-bounded dual jet flow, Int. J. Thermofluid. 26 (2025) 101125.

[20] P.J. Murphy, S. Alimohammadi, S.M. O'Shaughnessy, Experimental investigation of a wall-bounded dual jet flow for varying Reynolds number: Flow visualisation, hydrodynamic characteristics, and associated heat transfer, Int. J. Therm. Sci. 211 (2025) 109699.

[21] Y.A. Altaharwah, C.M. Hsu, Flow and mixing characteristics of single-pulsed dual parallel plane jets. Results in Engineering, 25 (2025) 103741.

[22] S. Kumar, S. Murugan, Investigation of flow characteristics and velocity fields of excited two parallel plane jets, Phys. Fluids. 36 (2024) 015142.

[23] T. Mondal, N. Hnaien, M. Ajmi, K. Ghachem, L. Kolsi, CFD Investigation of Thermal Characteristics for a Dual Jet with a Parallel Co-flow, ACS Omega 7 (2022) 27864−27875.

[24] W. Xu, R. Dong, S. Liang, Numerical simulation study of energy separation in jet shear layer, Process. 12:2 (2024) 331.

[25] A. Amamou, A. Elkaroui, R. Ben Khalifa, N.M. Said, H.I. El-Saeedy, Computational investigation of highly heated homogeneous subsonic turbulent jets issuing from plane and circular nozzles, Int. J. Therm. Sci. 187 (2023) 108163.

[26] ANSYS Fluent Theory Guide, ANSYS, Inc., 275 Technology Drive Canonsburg, PA 15317, July 2021.

[27] A. Assoudi, S. Habli, S.N. Mahjoub, H. Bournot, G. Le Palec, Experimental and numerical study of an offset jet with different velocity and offset ratios, Eng. Appl. Comput. Fluid. Mech. 9:1 (2015) 490-512.

[28] X.K. Wang, S.K. Tan, Experimental investigation of the interaction between a plane wall jet and a parallel offset jet, Exp. Fluids. 42:4 (2007) 551–562.